Journal of
Nanoelectronics and Optoelectronics
Vol. 1, 39–51, 2006

Deterministic Single-Photon and Polarization-Correlated Photon Pair Generations From a Single InAlAs Quantum Dot

Hidekazu Kumano[1,*], Satoshi Kimura[1], Michiaki Endo[1], Hirotaka Sasakura[2], Satoru Adachi[2,3], Shunichi Muto[2,3], and Ikuo Suemune[1,3]

[1]*Research Institute for Electronic Science, Hokkaido University, Sapporo 001-0021, Japan*
[2]*Department of Applied Physics, Hokkaido University, Sapporo 060-8628, Japan*
[3]*4–1-8, Hon-cho, Kawaguchi-shi, Saitama 332–0012, Japan*

(Received 28 January 2006; accepted 1 March 2006)

Photon emission with nonclassical photon statistics is discussed with a single InAlAs quantum dot. The deterministic single-photon generation in which the emitted photon wavelength matches well to the highly sensitive wavelength region of highly efficient, low-noise Si-single-photon detectors and also to an atmospheric transmission window is demonstrated. Competing transition processes between neutral and charged exciton species originating from an exclusive formation in the same single quantum dot are clarified. It was found that suppressing the charged exciton formation is possible by a quasi-resonant excitation for a deterministic monochromatic single-photon generation. Polarization-dependent photoluminescence spectroscopy clearly indicates the preservation of photon polarizations between photons emitted by biexciton/exciton recombinations. Furthermore, the deterministic polarization-correlated photon pair generation with biexciton-exciton cascaded transition occurring in a single quantum dot is directly confirmed by the polarized second-order photon correlation measurements. This indicates a longer polarization flip time than the exciton lifetime, which is an essential requirement for the deterministic Einstein-Podolsky-Rosen photon pair generation under the present biexciton-exciton cascaded transition scheme.

CONTENTS

1. INTRODUCTION

After an introduction of the first complete protocol by Bennett and Bastard in 1984,[1] quantum key distribution (QKD) has attracted a lot of attention since the absolutely secure key exchange guaranteed by fundamental quantum mechanical principles is feasible.[1–4] In 1991, another important protocol was invented by Ekert[5] and is based on purely nonclassical Einstein-Podolsky-Rosen (EPR) correlations.[6] Since any information will be encoded on these single or EPR photons in QKD, generation of single photons or ''entangled'' EPR photon pairs is a fundamental requirement for an implementation of QKD based on BB84[1,2] and E91[5,7] protocols, respectively.

At present, weak coherent pulse (WCP)[8–16] and entangled photons generated by nonlinear optical processes such as spontaneous parametric downconversion (SPDC)[17–21] are used as light sources, both of which provide photons in coherent state. Thus, inherent photon number fluctuation is inevitable, and photon generation essentially becomes probabilistic. In the case of BB84, for example, this will cause a low QKD rate since most of the pulses are empty. More important, the WCP can be never completely robust against a so-called beamsplitter attack due to residual multiphoton emissions regardless of a selection of average photon

*Author to whom correspondence should be addressed.

Hidekazu Kumano received his M.S. degree in Science from Hokkaido University, Japan, in 1996. He received the degree of Doctor (Engineering) from the Hokkaido University, Japan, in 2004. He worked as a researcher in SHOWA DENKO K.K. from 1996 to 1997. In April 1997, he joined Research Institute for Electronic Science (RIES) of the Hokkaido University as a research associate. He has worked on the growth and structural/optical characterization of wide bandgap, low-dimensional systems such as ZnSe/MgS superlattices and CdS quantum dots and engaged in the excitonic interaction with radiation field and phonon coupling, including a coupling between electronic systems and photonic fields in three-dimensional optical microcavities formed by electron-beam lithography and selective growth technique. He has also studied the fundamental optical properties of bulk GaN- and ZnO-related materials for novel light-emitting devices. His recent research interests are in the area of quantum information science and the physics of zero-dimensional semiconductors, especially for their nonclassical photon emission properties.

Satoshi Kimura received a bachelor's degree inf Engineering in 2004 from Hokkaido University. Currently, he is pursuing his master's degree in the Graduate School of Information Science and Technology, Hokkaido University. The subject of his thesis is "Photon Anti-Bunching Observation from Single InAlAs Quantum Dot."

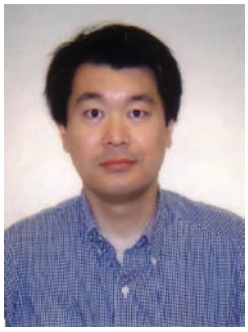

Michiaki Endo received his M.E. degree and Dr. degree in Electrical Engineering from the Muroran Institute of Technology, Japan, in 1994 and 1997, respectively. He had worked in Advantest Laboratories Ltd. from 1997 to 2003 for development of a surface contamination inspection apparatus on the semiconductor wafer. He joined the Research Institute for Electronic Science of Hokkaido University in 2004, where he engaged in the research and fabrication of nanostructures for semiconductor single-photon devices. He is a member of the Japan Society of Applied Physics.

Hirotaka Sasakura received his Ph.D. degree in Applied Physics from Hokkaido University, Japan, in 2003. He received a post-doctoral fellowship from the Japan Society for the Promotion of Science (JSPS) and worked as a Research Engineer in the Department of Applied Physics at Hokkaido University from 2002 to 2004. In April 2004, he joined the project in CREST, Japan Science and Technology Agency, where he is a Research Engineer. Dr. Sasakura's research interests are in the area of designing for quantum information processing. Current research topics include optical spin control in semiconductor nanostructures.

Satoru Adachi received his Ph.D. degree in Electrical Engineering from Osaka University, Japan, in 1991. He worked as a Research Associate in the Department of Material Science of Himeji Institute of Technology from 1991 to 2000. In April 2000, he joined the Department of Applied Physics of Hokkaido University, Japan, where he is an Associate Professor. In 1996–1997, he worked as a Visiting Scientist under Professor Keith A. Nelson at Massachusetts Institute of Technology, USA. Professor Adachi's research interests are in the area of spintronics in nanostructures. Current research topics in his group include coherent control of excitons and biexcitons in quantum dots and wide bandgap semiconductors and optical pumping of nuclear spin polarization in a quantum dot.

Shunichi Muto received his Ph.D. degree in Physics from the Tokyo Institute of Technology, Japan, in 1978. He worked as a research associate at Boston University and Washington University from 1978 to 1981, and as a researcher at Fujitsu Laboratories, Ltd., from 1981 to 1995. In 1995, he joined the Department of Applied Physics of Hokkaido University, Japan, as an Associate Professor, where, since 1997, he is a full Professor. Professor Muto's research interests are in the area of physics and applications of semiconductor nanostructures. Current research topics in his group include quantum computation using electron spins, coherent control of excitons and biexcitons in quantum dots, and wide bandgap semiconductors and optical pumping of nuclear spin polarization in a quantum dot. More information on his research can be found at http://www.eng.hokudai.ac.jp/labo/semi/index_english.html

Ikuo Suemune received his M.S. degree in Physical Electronics from the Tokyo Institute of Technology (TIT), Japan, in 1974. He received his Doctor degree in Physical Electronics from the Tokyo Institute of Technology in 1977. He worked as a Research Associate in the Faculty of Engineering of the Hiroshima University from 1977 to 1983 and as an Associate Professor from 1983 to 1993. In April 1999, he joined the Research Institute for Electronic Science of the Hokkaido University, Japan, where he is a Professor. He leads the Nanophotonics Laboratory, which is now located in the Nanotechnology Research Center of Hokkaido University. From 1986 to 1987 he was a Visiting Professor at the University of California, Santa Barbara, USA. Professor Suemune's research interests are in the area of nanophotonics, nanostructures, and nanodevices. Current research topics in his group include III-V-N related quantum dots, wide bandgap quantum dots, related single dot spectroscopy, semiconductor microcavities, and applications to quantum information communications. He has authored more than 260 refereed journal publications, more than 30 invited talks in international conferences, and 13 invited book chapters.

number per pulse. Actually, simple calculation shows that the zero photon probability $P(n=0)$ under a mean photon number per pulse μ_{WCP} is expressed as $P(0) \cong 1-\mu_{WCP}$, while the multiphoton probability as $P(n>1) \cong \mu_{WCP}{}^2/2$ when the μ_{WCP} is low enough.[22] On the other hand, in striking contrast to the coherent light, photons in a number state have a purely quantum nature as a consequence of full quantization of the radiation field, in which no photon number fluctuation is involved.[23]

To overcome these critical issues, therefore, deterministic single or entangled photon sources that will emit photons in the number state are necessary. Until now, deterministic single-photon emission has been demonstrated in several systems, such as single atoms,[24,25] single molecules,[26] nitrogen-vacancy centers in diamonds,[27] gold nanoclusters,[28] semiconductor nanocrystals,[29–31] and epitaxially grown single semiconductor quantum dots (QDs).[32–42] Among them, epitaxially grown semiconductor QDs are the most promising because of their stability, high photon emission rates, current-driving capabilities,[36] well-established semiconductor technologies, and availability of multiexciton states that is essential for the entangled photon pair generation.

From a historical viewpoint, research on the deterministic entangled photon sources is still in an early stage. In fact, the first demonstration of deterministic entangled photon pair generation from a QD has been reported recently.[43] Concerning the deterministic single-photon sources with QD systems, distinguished progress has been achieved[32–42] since the first report in 2000 by Michler et al.[32]

So far, in terms of a photon wavelength, almost all research focused on telecommunication wavelength applicable to QKD in fiber link[27–32] except for the materials with a wide bandgap [40–42] toward higher temperature operation. However, for realizing a flexible and expandable secure network system, free-space QKD will be of prime importance as a complementary link to the fiber network.[22,44] In the case of free-space QKD, photon wavelength should be tuned to a high atmospheric transmission window (i.e., around 770 nm)[45,46] to minimize the channel loss.

Another beneficial point of free-space QKD is that, unlike the fiber link, high-efficiency, low-noise Si single-photon detectors (SPDs) are available. Furthermore, atmosphere is not birefringent at optical wavelengths,[47] and thus photon polarization is well preserved during transmission. This fact allows us to implement a simple polarization encoding for the key distribution.

By virtue of these novel advantages, free-space QKD is solely a unique system that can provide the highest secure communication over line-of-sight paths, including ground to satellite.[48] Despite several pioneering works along this direction,[48–52] research on free-space QKD is still based on the classical Poissonian photon sources since so far no quantum photon sources applicable to the free-space QKD are available. Therefore, deterministic single or entangled photon sources applicable to the free-space link are strongly demanded.

In this article, photon emission with nonclassical photon statistics is discussed with a single InAlAs QD based on our recent results. The deterministic single-photon generation with the InAlAs QD was achieved for the first time. Emitted photon wavelength was well coincident with the highly sensitive region of highly efficient and low-noise Si SPDs together with atmospheric transmission window. Photon emission processes of neutral and charged excitons were shown to be exclusive and did not take place simultaneously in the same single QD. It was found that selective formation of neutral excitons is possible by a quasi-resonant excitation, which enhances highly monochromatic nonclassical single photon generation. Furthermore, polarization-correlated photon pair generation was also demonstrated using a biexciton-exciton cascaded transition (BECT) process, that is, $|XX> \rightarrow |X> \rightarrow |0>$, which strongly encourages a realization of the polarization-entangled photon pair generation.

2. FABRICATION AND CHARACTERIZATION OF SINGLE INALAS QUANTUM DOT

To implement highly efficient deterministic photon sources suitable for a free-space quantum channel, the emission wavelength of the semiconductor QD should be adjusted to the wavelength region with high atmospheric transmission and high sensitivity for SPDs. For this purpose, InAlAs QDs[53–55] are quite promising since the moderate Al incorporation into the well-established InAs

QD will cover the required wavelength region, and high luminescence efficiency is also expected.

The QDs sample was grown on a (001) GaAs substrate by molecular beam epitaxy. It had two-stacks of QD layers made of $In_{0.75}Al_{0.25}As$ and $In_{0.7}Ga_{0.3}As$ separated by an 11-nm thick $Al_{0.3}Ga_{0.7}As$ layer.[56] These QDs were prepared in Stranski-Krastanow (S-K) growth mode on $Al_{0.3}Ga_{0.7}As$ layers and were sandwiched with $Al_{0.3}Ga_{0.7}As$ layers. The topmost surface was terminated with a GaAs cap layer. Since coupling effects between adjacent QD layers separated by the 11-nm thick $Al_{0.3}Ga_{0.7}As$ spacer layer were almost negligible,[57] we focus on the $In_{0.75}Al_{0.25}As$ QDs.

Figure 1 shows photoluminescence (PL) spectrum from the macroscopic region of $In_{0.75}Al_{0.25}As$ QDs at 22 K. It was found that inhomogeneously broadened PL spectrum with about 90 meV full width at half maximum (FWHM) covers the wavelength region with high atmospheric transmittance and high sensitivity of SPDs. The additional structure found at around 730 nm stems from the wetting layer (WL) belonging to the S-K QD. After the growth, the sample was etched into mesa structures with the top lateral size of about 150 nm for isolating a single QD.

A scanning electron microscopy image of typical mesa structure is shown in the inset of Figure 2b, and the details of this sample preparation are described in Ref. 56. A mode-locked Ti:sapphire laser at a 730-nm wavelength with the pulse width 80 fs and a pulse repetition frequency of 82 MHz was used for pulsed excitations, a He-Ne laser at a wavelength of 632.8 nm, and a continuous wave (CW) Ti:sapphire laser were used for CW excitations. An objective lens with a numerical aperture (NA) of 0.5 and a magnification of 50× focused the laser beam on one of the mesa structures and collected luminescence emitted from several QDs in the mesa. Collected luminescence was dispersed by a 0.5-m single monochromator or a 0.64-m triple monochromator and was detected with Si charge coupled device (CCD) detectors or a streak camera. For evaluating photon statistics of emitted photons from a single QD, photon correlation measurements were employed by a Hanbury-Brown and Twiss (HBT) setup[58] with auto- and cross-correlated configurations. The data were taken at 22 K or 4 K.

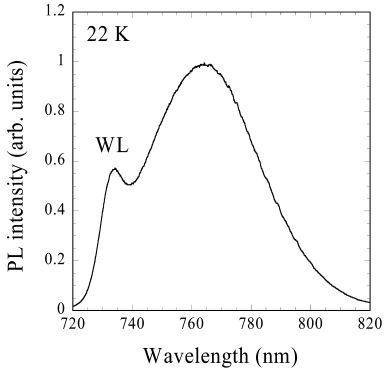

Fig. 1. Macroscopic PL spectrum of Stranski-Krastanow InAlAs QDs at 22 K. Inhomogeneous broadening is around 90 meV. Emission from wetting layer is observed at about 730 nm.

3. NONCLASSICAL SINGLE-PHOTON GENERATIONS

One of the fundamental aspects of semiconductor QDs is their atomiclike discrete energy spectrum. However, QDs exhibit quite rich physics compared to natural atoms, for example, effects of dot size and shape variation,[59–64] local field,[62,65,66] continuum state,[67–69] and charged species.[61,70–74] Therefore, the origins of emission lines are not self-evident, and transition energies differ dot to dot. Since the quantum photon sources are based on a recombination of excitonic complexes, understanding the electronic-level structure and identification of emission lines from our "artificial atom"[75,76] is essential for the implementation of the nonclassical photon sources.

Figure 2a shows a streak image obtained from a single InAlAs QD under WL excitation at the excitation power P_{ex} of 2 μW. The corresponding time-integrated PL spectrum is illustrated in Figure 2b. Several sharp emission lines (L1–L4) were well resolved. Although the energy positions of these emission lines are different from dot to dot, a series of emission lines in which the energy separation is around 4–5 meV was observed in most QDs. L1 and L3 emission lines, with energy separation of 4.5 meV as shown in Figure 2, are the typical case. Thus, the two

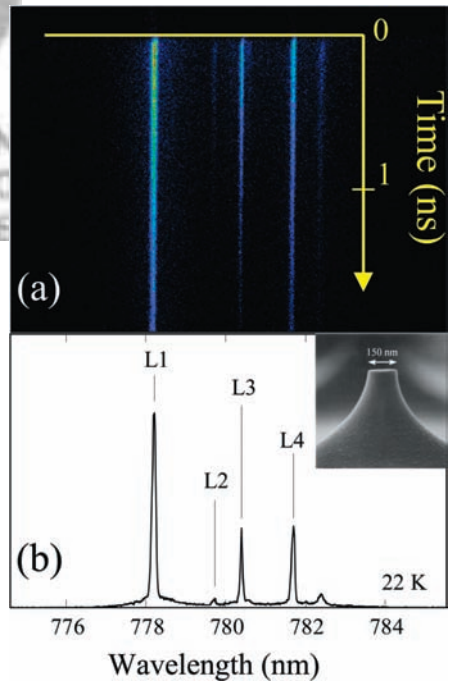

Fig. 2. (a) Streak image of emission lines under WL excitation. (b) Time-integrated PL spectrum corresponding to the streak image. Several emission lines denoted by L1 to L4 are observed. Scanning electron microscopy image of typical mesa structure employed in this study is also shown in the inset.

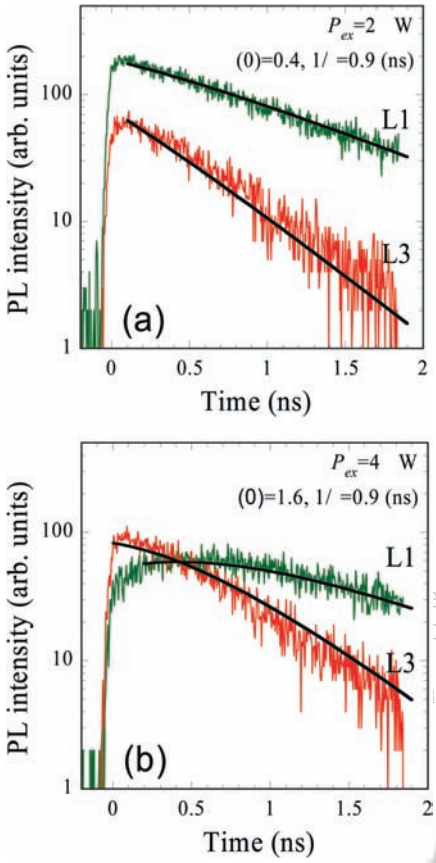

Fig. 3. PL decay curves for L1 and L3 lines under excitation power of (a) 2 μW and (b) 4 μW. Solid lines are fitted results, which give initial average exciton number μ(0) in a QD. The values of μ(0) = 0.4 and 1.6 for the excitation power of 2 μW and 4 μW, respectively, are estimated under the constant characteristic decay rate of $\gamma = 0.9\,\mathrm{ns}^{-1}$ (see text).

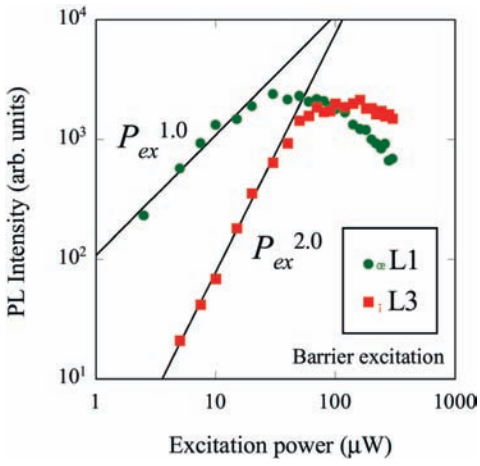

Fig. 4. Excitation power dependence for L1 (green circles) and L3 (red squares) emission lines under CW excitation.

emission lines L1 and L3 are discussed first, and emission lines L2 and L4 are discussed in Section 4.

Decay curves of both lines L1 and L3 are shown in Figure 3 for two excitation powers. Under $P_{ex} = 2$ μW, both lines show single exponential decay after a sharp rise, and lifetimes of 1.02 and 0.55 ns were obtained for L1 and L3 lines, respectively. Under $P_{ex} = 4$ μW, rise time became apparent in L1, and crossover of PL intensities was also observed. These observed behaviors under off-resonant excitation are well explained by a model presented by Santori et al.[77] In this model, an initial exciton population in a QD is assumed to have Poisson distribution $P(n) = \mu(0)^n exp(-\mu(0))\ /n!$, where n is a photon number per pulse, μ(0) is an initial mean exciton number in a QD, and time evolution of biexciton and exciton PL intensities are assumed to be of the form $I_X(t) = \gamma I_0 P_n(t)$ and $I_{XX}(t) = 2\gamma I_0 P_n(t)$, respectively, where γ is a characteristic decay rate, I_0 is a constant expressing the collection efficiency, and $P_n(t)$ is a probability of finding n excitons in a QD at a time t under a uniform decay of mean exciton number as $\mu(t) = \mu(0)\exp(-\gamma t)$. The thick solid lines in Figure 3 are fitted PL intensity evolutions for these two excitation powers with the common characteristic decay rate of $\gamma = 0.9\,\mathrm{ns}^{-1}$.

From this analysis, initial mean exciton numbers in a QD, $\mu(0) = 0.4$ and 1.6 were estimated for $P_{ex} = 2$ and 4 μW, respectively. Excitation power dependence of L1 and L3 was examined with CW excitation, and linear and bilinear increases of the PL intensity with the higher excitation power were observed as shown in Figure 4, which are the characteristic features of exciton and biexciton recombinations, respectively. Besides, both lines exhibit fine-structure splittings discussed in more detail below. Therefore, these results ensure that L1 and L3 peaks originate from neutral exciton X^0 and biexciton XX^0 emissions, respectively. This discussion suggests that the neutral exciton and biexciton recombination events take place in the same QD.

In the following, nonclassical single photon emission is investigated by second-order photon correlation measurements. A direct way to evaluate the statistics of emitted photon is just "counting" of the number of photons per excitation cycles. However, such a photon counter that can distinguish different photon numbers with high efficiency is now under development[78] and not commercially available. In this work, therefore, Si-avalanche photodiodes were employed as SPDs, and the second-order photon correlation function $g^{(2)}(\tau)$ was measured with HBT setup[58] to determine the photon statistics.

In Figure 5, our experimental setup is presented. Collected luminescence from a QD is divided into two beams by a 50/50 beamsplitter. Each beam is then dispersed by a 0.2-m monochromator (MC1 and MC2) and a single emission line is filtered with 1-nm FWHM transmission bandwidth. The transmitted photons are introduced into each SPD through optical fibers. Each time a photon is detected in one of the detectors, an electronic pulse is produced and sent to a time-to-amplitude converter (TAC). The outputs of SPDs serve as start and stop signals for correlation measurement. The temporal difference between the two

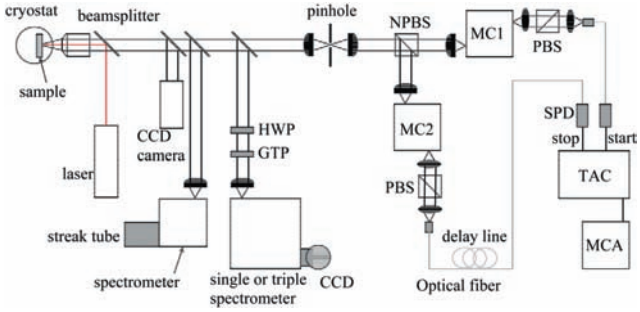

Fig. 5. Overall experimental setup. CCD imaging camera, streak camera, CCD detector, and HBT setup can be switched by flipper mirrors. Half-wave plate (HWP) and Glan-Thomson polarizer (GTP) are used for polarization-dependent PL measurements. Polarized beamsplitters (PBSs) after spectral filtering are for the polarization-dependent photon correlation measurements. Sample temperatures were 4 K or 22 K.

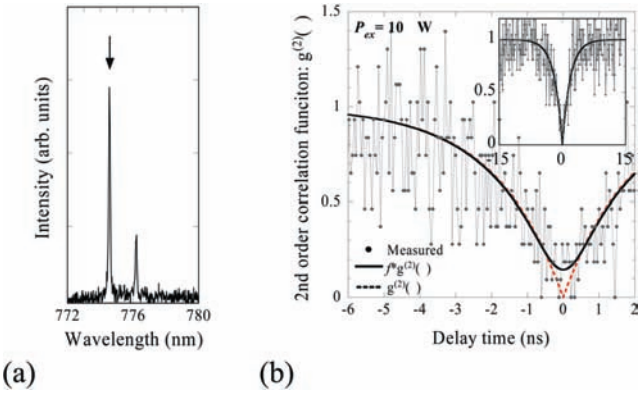

Fig. 6. (a) PL spectrum of the QD employed in the CW-excited photon correlation measurements. The excitonic transition line (774.4 nm) was introduced into the HBT setup, and photon statistics were measured. (b) Resultant second-order correlation function $g^{(2)}(\tau)$ at around zero time delay measured at the excitation power of 10 μW. Solid line shows an $f*g^{(2)}(\tau)$ curve to give the best fit to the measured data, and the red dashed line is a deconvoluted second-order correlation function $g^{(2)}(\tau) = 1 - \alpha \exp[-(G + 1/\tau_1)\tau]$. Inset shows the $g^{(2)}(\tau)$ profile in the extended time range.

outputs, which is defined as $\tau = t_{stop} - t_{start}$, is translated into a pulse height. Finally, 13-bit multichannel analyzer (MCA) accumulates the single event data and produces histograms of the number of counts as a function of the delay time τ. The overall temporal resolution of the setup is estimated to be 1 ns, limited by the time jitter of the detectors. By selecting the photon wavelengths on each path, photon correlation function can be measured under both autocorrelation and cross-correlation configurations.

Experimentally, normalized second-order correlation function, defined as $g^{(2)}(\tau) = \langle I(t)I(t+\tau)\rangle / \langle I(t)\rangle^2$, where $\langle I(t)\rangle$ is an expectation value of the intensity at time t,[23] is readily constructed by measuring the joint probability of detecting arrival time of one photon at time t and another photon at time $t + \tau$ as long as τ is much smaller than the mean time between detected events.[79] This condition is always satisfied throughout this article, and the second-order correlation functions were directly measured through the intensity correlation.

At first, photon statistics of emitted photons from a single InAlAs QD were studied under CW excitation. The PL spectrum of this sample is shown in Figure 6a, and an excitonic transition at a wavelength of 774.4 nm, denoted by an arrow, was used for the photon correlation measurements. Detailed description of the optical properties on this sample is given in Refs. 80 and 81. Figure 6b shows a measured second-order correlation function $g^{(2)}(\tau)$ at around zero time delay, whereas the extended time range profile is shown in the inset. In this experiment, excitation power was 10 μW, which corresponds to a steady-state exciton population in a QD of less than 0.1[81] from a rate equation analysis with the four-level ladder model.[82] It is obvious that the correlation count at $\tau = 0$ is strongly suppressed. This photon antibunching behavior, des cribed by $g^{(2)}(0) < 1$, is a clear manifestation that the photons emitted from the InAlAs QD have purely a quantum nature.[23] Since the correlation function at zero time delay, what we call *coincidence count*, is expressed as $g^{(2)}(0) = 1 - 1/n$ for n photon number state, observed $g^{(2)}(0) \sim 0$ indicates that one and only one photon emission (i.e., single-photon emission) in number state ($n = 1$) is realized. This is a first demonstration of nonclassical single-photon emission from the single InAlAs QD, which will be applicable to the nonclassical photon sources for free-space channel.

It is found that the measured correlation function is well fitted by a convoluted curve $f*g^{(2)}(\tau)$, indicated by the solid line in Figure 6b, where f is the time response function of our experimental setup,[80] and $g^{(2)}(\tau)$ is expressed as $g^{(2)}(\tau) = 1 - \alpha \exp[-(G + 1/\tau_1)\tau]$.[79] Here, α is a fitting parameter phenomenologically introduced to give a purity of single-photon emission, G is the excitation rate, and τ_1 is the exciton lifetime. The red dashed line exhibits the correlation function $g^{(2)}(\tau)$ used in the present fitting procedure, and as a result, α is estimated to be unity. To realize highly efficient single-photon emitters, sufficient exciton population in a QD is necessary to reduce the probability to emit zero photons. Therefore, excitation power dependence of the photon antibunching properties is examined.

The α values measured as a function of the excitation power are summarized in Figure 7. It will be clear that the α value remains almost unity under the weak excitation condition up to the CW excitation power of 50 μW, which corresponds to a steady-state exciton population in a QD of about 0.4. This result definitely indicates that the highly pure regulated single-photon emission is possible in the relatively weak excitation range. With the higher excitation above this critical excitation power, however, the α value was substantially decreased, and single-photon emission properties were degraded due to the interactions between multiexciton states and the exciton state under high excitation powers.[81]

For a confirmation of deterministic single-photon emission per pulsed excitation, autocorrelation measurements

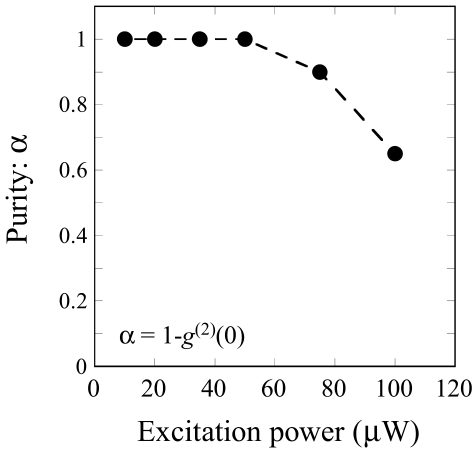

Fig. 7. Purity of single-photon emission as a function of excitation power.

under pulsed excitations were performed with the same QD given in the Figure 2. The X^0 line in the inset of Figure 8, which corresponds to the L1 line in Figure 2b, was introduced into the HBT setup. The excitation power was set to satisfy the condition on an average initial exciton number $\mu(0) < 1$, and the resultant correlation function is illustrated in Figure 8. In this measurement, the time window of TAC was 200 ns, and the signal was integrated over 1800 s. The observed peak period of about 12.2 ns corresponds to an excitation pulse repetition of 82 MHz. As observed in the CW excitation, a strongly suppressed coincidence count of $g^{(2)}(0) \sim 0$ was measured under the pulsed excitation. Deterministic single-photon emission per excitation pulse from the single InAlAs QD is now unambiguously confirmed by the photon correlation measurements.

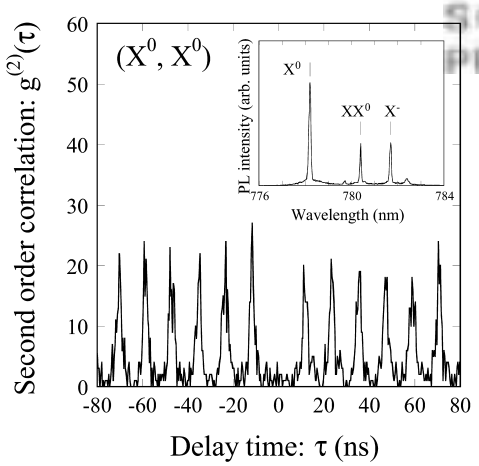

Fig. 8. Result of autocorrelation measurement for the X^0 line in the same QD shown in Figures 2–4. The Ti:sapphire laser with a wavelength of 730 nm was used for the excitation. Observed peak separation of about 12.2 ns corresponds to an excitation laser frequency of 82 MHz. Clear photon antibunching is observed at $\tau = 0$. Inset shows assignment of emission lines in QD1.

4. COMPETING TRANSITION PROCESSES IN A SINGLE QUANTUM DOT

In this section, the competing transition processes in a single QD and the control of these processes are discussed with respect to the remaining L4 and L2 emission lines shown in Figure 2. In terms of PL lifetime and excitation power dependence measurements, the L4 line showed excitonic behavior, that is, the measured lifetime was about 0.9 ns with weak excitation, and its PL intensity was linearly dependent on the excitation power. For further studying the L4 line, nonpolarized high-resolution PL measurements and polarization-dependent PL measurements were employed under the WL excitation with CW Ti:sapphire laser at 4 K. For the polarization-dependent PL measurements, a rotatable half-wave plate followed by a horizontal polarizer were placed in front of an entrance slit of a 0.64-m triple monochromator as shown in Figure 5, and the rotational angle dependence of the luminescence was continuously measured under the linear basis ($V = 0°$) of polarization detection with respect to the principal in-plane crystal axes.

In the higher-resolution PL spectrum measurements shown in Figures 9 and 10, the L4 line (781.553 nm; 1.58633 eV) remains as a single peak within the spectral resolution of about 15 μeV. Moreover, no polarization dependence was detected in the polarization-dependent PL measurements, as shown in Figure 10a. These results attribute the origin of the L4 line to the trion state,[61] possibly negatively charged excitons (X^-) in terms of the positive binding energy relative to the neutral exciton.[55, 72, 83] Associated with the negatively charged excitons, a negatively charged biexciton that is composed of three electrons and two holes confined in a QD is also expected from an analogy with the neutral biexciton. In a high-resolution spectrum measurement shown in Figure 9, the L2 line exhibits a doublet structure composed of $L2_a$ (779.560 nm; 1.59038 eV) and $L2_b$ (779.616 nm; 1.59027 eV) lines. Energy separation is 110 μeV, which is strongly dependent on the dot size. The L2 line has a lifetime of 0.47 ns, and the luminescence intensity has a bilinear dependence of about $P_{ex}^{2.1}$. Hence, the L2 lines are assigned to be the negatively charged biexciton (XX^-), and the observed splitting is attributed to the isotropic electron-hole (*e-h*) exchange interaction in the excited trion state,[84] which shows dot-size

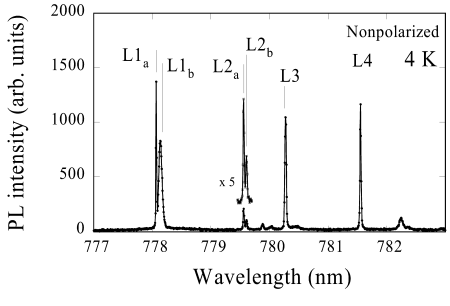

Fig. 9. High-resolution PL spectrum at 4 K.

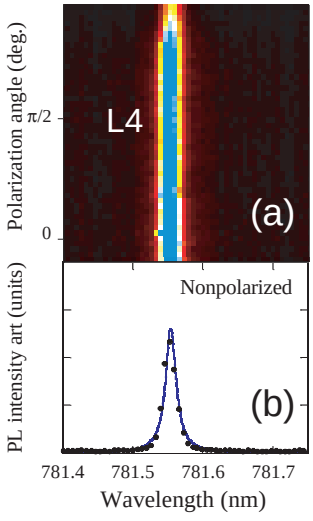

Fig. 10. Polarization-dependent PL spectrum of L4 emission line. Fine structure splitting is absent within the spectral resolution of about 15 μeV. The solid line is a fitted spectrum with a Lorentzian function.

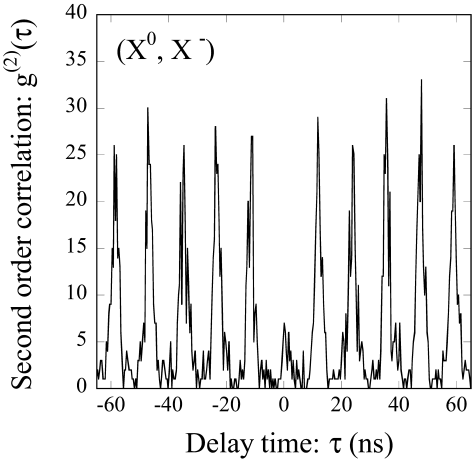

Fig. 11. Crossed photon correlation measurement under (start, stop) = (X^0, X^-) configuration. Suppressed coincidence count indicates that the X^0 and X^- emissions are from the same QD, and that neutral and charged species are formed exclusively with each other, which leads to competing transition processes between $|XX> \rightarrow |X> \rightarrow |0>$ and $|XX^-> \rightarrow |X^-> \rightarrow |e^->$.

dependence, reflecting the probability that the first or the second excited electron and the trion hole occupy the same position.[61]

To reveal the mutual relations between neutral and charged excitons, the photon correlation function was measured under (start, stop) = (X^0, X^-) configuration. As a result, clear antibunching was observed as shown in Figure 11. The adjacent periodic correlation peaks represent an X^0 photon emission by one laser pulse and subsequent X^- photon emission by the next pulse after a 12.2-ns interval. The observed antibunching directly exhibits that the two emission lines X^0 and X^- originate from the same single QD,[85,86] and that neutral and charged excitons are formed exclusively with each other in the same QD.

This competing behavior is also reflected in a steady-state PL property. Excitation power dependences of the PL intensities for X^0 (open squares), X^- (crosses), XX^0 (open triangles), and XX^- lines (open circles), and the summed intensities of $X^0 + X^-$ (green squares) and $XX^0 + XX^-$ (red circles) are shown in Figure 12a. The PL intensities as a function of excitation power were analyzed by applying a ladder model,[82,85] which is composed of 0–3 excitonic multiplex states as depicted in Figure 12b. By solving the rate equations, steady-state PL intensities I_x and I_{xx} are expressed as

$$I_X \propto \frac{p_1}{\tau_1} = \frac{1}{\tau_1}\left(1 + \frac{1}{G\tau_1} + \frac{G\tau_2}{2} + \frac{G^2\tau_2\tau_3}{2}\right)^{-1}, \quad (1a)$$

$$I_{XX} \propto \frac{p_2}{\tau_2} = \frac{1}{\tau_2}\left(1 + \frac{2}{G\tau_2} + \frac{2}{G^2\tau_1\tau_2} + G\tau_3\right)^{-1}, \quad (1b)$$

where τ_i is the radiative lifetime of the ith state, p_i is the probability of finding the ith excitonic multiplex in the QD, and G is an exciton excitation rate. The lifetimes of X^0 and XX^0 lines were fixed to the measured values of 1.02 and 0.55 ns, respectively, as measured in Figure 3a. The p-shell exciton decay time of about 0.3 ns was separately measured by a state-filling spectroscopy[87] with QD ensemble under sufficiently high pump power. Here, the biexciton excitation rate was assumed to be $1/2G$ because of the spin-selective exciton capture to form a bright biexciton. Calculated I_x and I_{xx} lines are given with the solid lines in Figure 12a, and the steady-state exciton population in one QD is shown in the upper axis. It is obvious that the present ladder model fits well for the total intensities of exciton ($X^0 + X^-$) and biexciton ($XX^0 + XX^-$) intensities rather than the single emission line intensities of neutral or charged species. In this fitting, the exciton excitation rate $G = 1\ \mathrm{ns}^{-1}$ corresponds to an excitation power

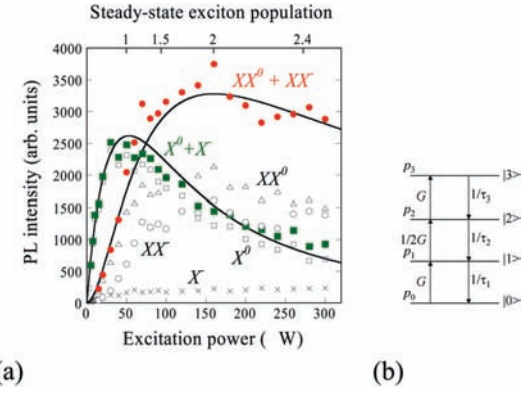

Fig. 12. (a) Excitation power dependence of PL intensities for X^0 (open squares), X^- (crosses), XX^0 (open triangles), and XX^- lines (open circles). Summed intensities of $X^0 + X^-$ (green squares) and $XX^0 + XX^-$ (red circles) are also shown. (b) Schematic picture of four-level ladder model used in the analysis.

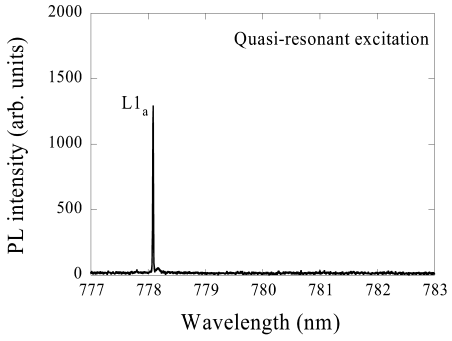

Fig. 13. Selective formation of a neutral exciton in a QD by a quasi-resonant excitation. Excitation energy is 23 meV above the emission energy. Charged exciton emission is almost absent.

of 38 μW. This result shows that the two neutral and charged exciton recombination processes are temporarily competing with each other, and the averaging in the steady-state luminescence measurements makes the combined intensities of $X^0 + X^-$ and $XX^0 + XX^-$ obey the above model. This, in another sense, gives support for the previous assignment of XX^-. The relative energy position of the XX^- peak (L2) in Figure 9 implies the negative binding energy of XX^- with respect to X^- (L4) and XX^0 (L3). The steady-state rate equation analysis and the photon correlation measurement in the (start, stop) = (X^0, X^-) configuration present the competing transition nature of $|XX^0> \rightarrow |X^0> \rightarrow |0>$ and $|XX^-> \rightarrow |X^-> \rightarrow |e^->$ in the same QD.

From a practical point of view, this uncontrolled two-color photon generation will result in a degradation of QKD quality, such as the decrease of the bit rate and probabilistic photon emission after spectral filtering. Therefore, higher control of charge states of an exciton formed in a QD is essential for the practical implementations to monochromatic and deterministic single-photon sources. In this regard, the population processes of excitons into a QD should be simplified, and the quasi-resonant excitation will prevent the additional carrier trap into a QD via a continuum states such as WLs and barrier layers. It is found that the neutral exciton can be selectively formed in the QD and shows dominant contribution to the PL spectra, while the charged exciton emission is almost absent, as shown in Figure 13. Although a detailed mechanism of the observed neutral exciton splitting into $L1_a$ (778.068 nm; 1.59343 eV) and $L1_b$ (778.134 nm; 1.59330 eV) line is not so far completely understood, this splitting is probably caused by the fluctuation of local field through the impurity state in the barrier layers.

5. POLARIZATION-CORRELATED PHOTON PAIR GENERATION

In the other sections, deterministic single-photon emissions from a single InAlAs quantum QD were demonstrated. Based on this significant progress of deterministic single-photon sources, generation of nonclassical EPR photon pairs, so-called entangled photon pairs,[6] is becoming more and more important.[88–90] So far, entangled photon pair generation has been mainly demonstrated with nonlinear optical processes in bulk, such as SPDC[17–21] and hyperparametric scattering (HPS).[91] However, in these schemes only probabilistic emission is possible due to a contribution of collective states rather than a single atomiclike quantum system. Since the entangled photon pair plays a central role in the novel large-scale quantum communications with a common synchronization signal, realization of deterministic entangled photon pair sources is a crucial and challenging issue. In this section, criteria for entangled photon pair generations are discussed, and our recent demonstration of polarization-correlated photon pair generation is reported, including the overview of the current status of research in this field.

The three schemes for the entangled photon pair generation (i.e., SPDC, HPS, and BECT) are schematically depicted in Figure 14, and their optical processes are compared. In contrast to the simultaneous photon pair generation in the SPDC and HPS processes caused by the second-order and third-order optical nonlinearities, respectively, the BECT is based on sequentially occurring linear optical processes. Therefore, polarization dephasing in the intermediate exciton states is probable, which will spoil the expected polarization correlation between photons emitted from biexciton-exciton transition processes. This process is suppressed when the polarization flip time is longer than the exciton lifetime, which is one of the requirements for the entangled photon pair generation with the BECT scheme. Because the polarization dephasing involves interactions with environments inherent to the solid-state systems,[92, 93] even though such effects are in general strongly suppressed in a QD[94, 95], this requirement can be a crucial issue. Actually, as far as we know, a polarization-correlated photon pair was observed only in the limited literature with InAs[96, 97] and CdSe[98] QDs, while no polarization correlations were observed from InAs QD in some literature.[99, 100]

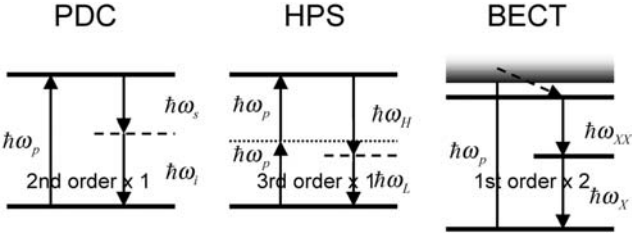

Fig. 14. Schematics of optical transitions in the spontaneous parametric down conversion (SPDC), hyper parametric scattering (HPS), and present biexciton-exciton cascaded transition (BECT) processes. In contrast to the nonlinear SPDC and HPS processes, the BECT is based on a sequential linear processes.

As the second important issue, exciton-level splittings due to anisotropic *e-h* exchange interactions will also cause a serious effect on the entangled photon pair generation.[43] When the two bright exciton states are degenerated as depicted in Figure 15a, generation of a polarization entangled photon pair is expected, in which the photon state is described as the entangled (Bell) state: $|\psi> = 1/\sqrt{2}$ ($|\sigma^+>_{XX}|\sigma^->_X + |\sigma^->_{XX}|\sigma^+>_X$), where $|>_{XX}$ ($|>_X$) denotes a photon state emitted by biexciton (exciton) recombination and σ^+ (σ^-) is a right (left) circular polarization. In this ideal case, transition energies of two decay paths are identical, and one cannot obtain the polarization information by observing the photon energies. Hence, "which-path information" is hidden. However, in the presence of state mixing caused by the anisotropic *e-h* exchange interaction between the bright exciton states, which is the case for lower symmetry than D_{2d}, degeneracy of bright exciton levels are lift off, as illustrated in Figure 15b.[59] Under this situation, the polarization information leaks to the photon energy; thus, the which-path information is disclosed, and the entangled state is no longer realized.

From the above discussion, the following two conditions should be satisfied to realize the entangled photon pair with the BECT scheme in a single QD system: (1) Polarization flip time of excitons is longer than exciton lifetimes, and (2) exciton homogeneous linewidths are wider than fine structure splittings between bright excitons, both of which are inevitable conditions for the polarization preservation and the hidden which-path information, respectively.

To confirm the optical BECT process experimentally, cross-correlation measurements under (start, stop) = (XX^0, X^0) configuration were carried out. In this case, excitation power was set to give $\mu(0) > 1.5$ for the sufficient count rate of biexciton emission, and the time window of TAC was set to 200 ns. Clear photon bunching behavior at $\tau = 0$

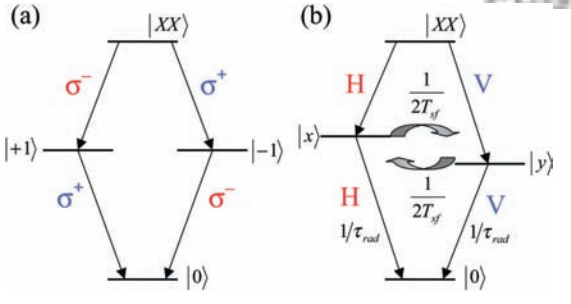

Fig. 15. Atomiclike energy levels formed in a (a) symmetric and (b) asymmetric QD. For a symmetric QD, two exciton levels, denoted by $|+1>$ and $|-1>$ are degenerated. In this case, generation of polarization-entangled photon state $|\psi> = 1/\sqrt{2}$ ($|\sigma^+>_{XX}|\sigma^->_X + |\sigma^->_{XX}|\sigma^+>_X$) is expected in the BECT scheme. On the other hand, for an asymmetric QD, two exciton states are a linear combination of the two angular momentum eigenstates, that is, $|x> = |+1> - |-1>$, $|y>| = |+1> + |-1>$, and therefore the degeneracy is lift off. This provides which-path information in their emisisons. Spin flip time of $1/(2T_{sf})$ between two exciton states is discussed in Section 5.

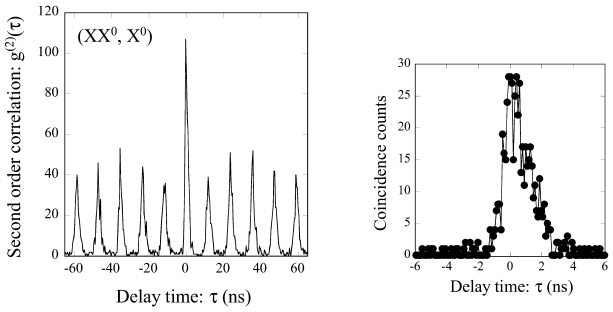

Fig. 16. (a) Second-order correlation function obtained by (start, stop) = (XX^0, X^0) configuration. (b) Close view of the correlation peak at zero time delay. The observed asymmetric line shape reflects the biexciton-exciton cascaded transition (BECT) occurring in a single QD.

was exhibited as shown in Figure 16a. This indicates that both the XX^0 and X^0 photons were emitted sequentially just after the excitation with laser pulses. To clarify the bunching behavior in more detail, the central peak was closely examined with a 50-ns TAC time window. As shown in Figure 16b, the correlation peak at the zero time delay displays asymmetric line shape; the abrupt rise near $\tau = 0$, followed by an exponential decay for the positive delay time was observed. This reflects that, after the excitation, the biexciton is formed in a QD, and the XX^0 photon emission accompanied with the biexciton decay takes place. Then, the exciton population is fed, and the X^0 emission follows. This sequence is consistent with the distinct rise time observed in the exciton emission line as shown in Figure 3b. The strongly suppressed coincidence count at $\tau < 0$ indicates, on the other hand, that the inverse order process is much less probable because the biexciton repopulation from the ground state in the QD is necessary after the exciton recombination.[101] Therefore, the observed photon bunching in the (XX^0, X^0) configuration unambiguously indicates a deterministic photon pair generation for each excitation pulse, which is expected by the energy-level structure in a QD as depicted in Figure 15.

For further investigation of the excitonic energy-level structure in a QD by means of spectroscopy, both nonpolarized and the polarization-dependent high-resolution PL measurements were performed for both the neutral biexciton (L3) and the exciton (L1a and L1b) lines. The results are summarized in Figure 17. It is clearly found that the nonpolarized PL spectra denoted by black curves are composed of two orthogonal linear-polarized components, indicated by red and blue curves obtained under 0° and 90° polarization angles, respectively. Furthermore, those two components show an anticorrelated behavior; that is, at the polarization angles where the longer wavelength component is dominant in XX^0, the shorter wavelength component is notable in X^0 and vice versa. The energy splittings between the two linearly polarized components are around

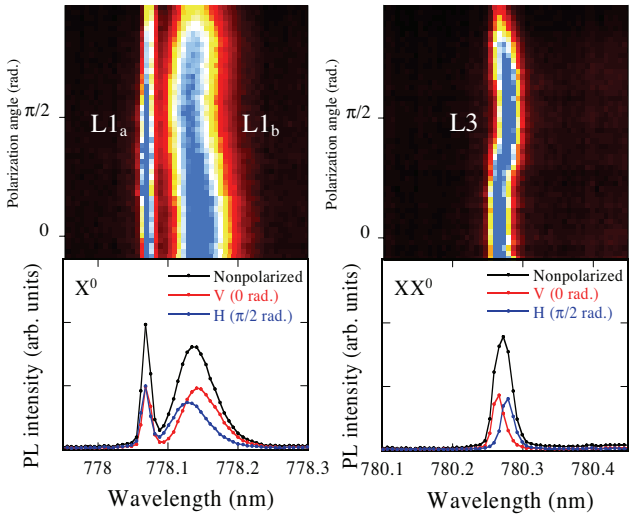

Fig. 17. Polarization-dependent PL spectrum of neutral exciton (L1) and biexciton (L3) emission lines. Black, red, and blue curves are non-polarized, vertically polarized, and horizontally polarized PL spectra, respectively. The energy splittings between the two linearly polarized components are around 30 μeV (= 0.0147 nm) for both the XX^0 and X^0 emission lines.

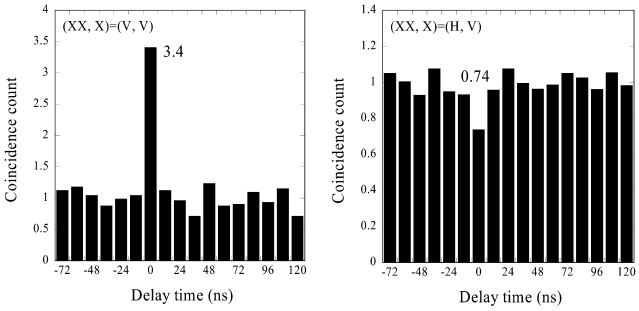

Fig. 18. Results of polarization-dependent photon correlation measurements for the XX^0–X^0 transition with (a) colinear and (b) cross-linear configurations.

30 μeV for both the XX^0 and X^0 emission lines. These results clearly indicate that the degeneracy between two bright exciton levels were lift off due to the anisotropic *e-h* exchange interaction,[59] and the fine structure splitting was sufficiently discerned, as is illustrated in Figure 15b.

With respect to the second condition for the entangled photon pair, the observed fine structure splitting should be lowered below the homogeneous broadening of around 5.5 μeV estimated by heterodyne four-wave mixing (FWM).[102] Since the anisotropic *e-h* exchange interaction between bright exciton states originates from the anisotropy of an exciton confinement potential, further improvement of QD growth condition or applying external fields will overcome this exciton-level splitting, which will lead to the disclosed which-path information.[43] The broadening of the homogeneous linewidth through the Purcell effect can be another promising approach to this problem.[103–105]

It should be stressed that, from a viewpoint of the first condition related to polarization preservation, the anticorrelated behavior observed in the polarization-dependent PL measurement strongly suggests an inefficient exciton spin flip in the timescale of exciton lifetime, while otherwise the polarization dependence will be lost in the X^0 emission. To investigate directly the polarization correlation between the XX^0 and X^0 photons emitted after each excitation pulse, polarization-dependent photon correlation measurements were carried out with the experimental setup shown in Figure 5. In the measurements, polarized beamsplitters are placed after each monochromator of MC1 and MC2 to select the photon polarizations. Colinear and cross-linear correlation were measured in (XX^0, X^0) = (V, V) and (H, V) configurations, respectively.

The obtained histograms are shown in Figure 18, where the coincidence counts were integrated for each correlation peaks. The area of the zero-delay peak is normalized to the average integrated area of the other peaks. The resultant zero-delay peak area for the colinear and cross-linear configurations was $C_{VV} = 3.4 \pm 0.5$ and $C_{HV} = 0.74 \pm 0.15$, respectively. Observed coincidence counts under colinear and cross-linear configurations show remarkable difference from the average value of unity, which indicates the polarization-correlated photon pair generation in the BECT scheme.

Exciton polarization flip time can be estimated based on the energy-level diagram as depicted in Figure 15b, including the exciton spin flip.[97] Probabilities of finding the exciton in $|x>$ and $|y>$ states at a time t, that is, $p_x(t)$ and $p_y(t)$ respectively, can be calculated from the rate equations:

$$\frac{dp_x}{dt} = \left(-\frac{1}{2T_{sf}} - \frac{1}{\tau_{rad}}\right)p_x + \frac{1}{2T_{sf}}p_y \qquad (2a)$$

$$\frac{dp_y}{dt} = \frac{1}{2T_{sf}}p_x + \left(-\frac{1}{2T_{sf}} - \frac{1}{\tau_{rad}}\right)p_y \qquad (2b)$$

where $2T_{sf}$ is the spin flip time, and τ_{rad} is the exciton recombination lifetime. Initial conditions are set as $p_x(0) = 1$ and $p_y(0) = 0$, and equal probability of the biexciton decay to the $|x>$ or $|y>$ state is assumed. Degree of correlation is defined as $\eta = (C_{VV} - C_{HV})/(C_{VV} + C_{HV})$, where $C_{\alpha\beta}$ is the coincidence count from the measurement in (XX^0, X^0) = (α, β) configuration. $C_{\alpha\beta}$ is given by calculating the joint probability of emitting a α-polarized photon for biexciton and a β-polarized one for exciton emission. Thus, using the polarization flip probability ε [= $1/2(1-\eta)$] the coincidence counts are expressed as $C_{VV} = \eta_{V,XX}\eta_{V,X}(1-\varepsilon)/2$ and $C_{HV} = \eta_{H,XX}\eta_{V,X}\varepsilon/2$, where $\eta_{H,XX}$ and $\eta_{V,X}$ are the polarization-dependent collection efficiencies of XX^0 and X^0 luminescence, respectively.[97] As a result, exciton spin flip time $2T_{sf} = \tau_{rad}(1-2\varepsilon)/\varepsilon = 3.6$ ns for the $\tau_{rad} = 1$ ns is obtained, which is consistent with the separately measured result from the FWM experiment with QD ensembles.[102] Therefore, the second condition (i.e., the polarization flip

time of excitons is longer than the exciton lifetime) is sufficiently satisfied. and the polarization preservation in the present BECT scheme is shown to be possible.

6. SUMMARY

Single-photon generation with nonclassical photon statistics from InAlAs QDs was demonstrated for the first time. Emitted photon wavelength is well coincident with the highly sensitive wavelength region of highly efficient and low-noise Si SPDs and with the atmospheric transmission window. Therefore, it is highly preferable for the implementation of a quantum light source for free-space QKD. The contribution of competing transition processes between exclusively formed neutral and charged exciton species in the same single QD was revealed. Selective formation of the neutral exciton was shown to be possible by the quasi-resonant excitation, which will lead to the realization of the monochromatic and deterministic single-photon sources. Polarization-correlated photon pair generation was also demonstrated using BECTs belonging to the same single QD. This demonstration directly implies the polarization preservation is possible in the timescale of exciton lifetime, which is quite encouraging for the deterministic polarization entangled photon pair generation. One of the remaining issues is suppressing the fine structure splitting of bright excitons for erasing the which-path information in the BECTs. As discussed by Stevenson et al.,[43] preparing the highly isotropic confinement potential by the further improvement of the QD growth condition or applying external fields could be a solution to this issue. The broadening of exciton homogeneous linewidth through a Purcell effect can be another promising approach to overcome this problem.[103–105]

Acknowledgments: We would like to acknowledge Dr. H. Z. Song, S. Hirose, and M. Takatsu for the sample preparation.

References

1. C. H. Bennett and G. Brassard, *Proc. IEEE Int. Conf. Comp. Sys. Signal Proc.*, Bangalore, India, 175 (**1984**).
2. C. H. Bennett, F. Bessette, G. Brassard, L. Salvail, and J. Smolin. *J. Cryptol.*, 5, 3 (**1992**).
3. B. Huttner and A. K. Ekert. *J. Mod. Opt.*, 41, 2455 (**1994**).
4. C. H. Bennett, G. Brassard, C. Crépeau, and U. M. Maurer, *IEEE Trans. Inf. Theory*, 41, 1915 (**1995**).
5. A. K. Ekert. *Phys. Rev. Lett.*, 67, 661 (**1991**).
6. A. Einstein, B. Podolsky, and N. Rosen. *Phys. Rev.*, 47, 777 (**1935**).
7. C. H. Bennett, G. Brassard, and N. D. Mermin. *Phys. Rev. Lett.*, 68, 557 (**1992**).
8. P. D. Townsend, J. G. Rarity, and P. R. Tapster. *Elec. Lett.*, 29, 634 (**1993**).
9. J. D. Franson and B. C. Jacobs, *Elec. Lett.*, 31, 232 (**1995**).
10. R. J. Hughes, G. L. Morgan, and C. G. Peterson, *J. Mod. Optics*, 47, 533 (**2000**).
11. A. Muller, H. Zbinden, and N. Gisin. *Europhys. Lett.*, 33, 335 (**1996**).
12. A. Muller, T. Herzog, B. Huttner, W. Tittel, H. Zbinden, and N. Gisin. *Appl. Phys. Lett.*, 70, 793 (**1997**).
13. H. Zbinden, J. D. Gautier, N. Gisin, B. Huttner, and A. Muller. *Elec. Lett.*, 33, 586 (**1997**).
14. G. Ribordy, J. D. Gautier, N. Gisin, O. Guinnard, and H. Zbinden. *Elec. Lett.*, 34, 2116 (**1998**).
15. C. Gobby, Z. L. Yuan, and A. J. Shields. *Appl. Phys. Lett.*, 84, 3762 (**2004**).
16. T. Kimura, Y. Nambu, T. Hatanaka, H. Kosaka, and K. Nakamura. *Jpn. J. Appl. Phys.*, 43, L1217 (**2004**).
17. C. K. Hong, Z. Y. Ou, and L. Mandel. *Phys. Rev. Lett.*, 59, 2044 (**1987**).
18. Y. H. Shih and C. O. Alley. *Phys. Rev. Lett.*, 61, 2921 (**1988**).
19. T. E. Kiess, Y. H. Shih, A. V. Sergienko, and C. O. Alley. *Phys. Rev. Lett.*, 71, 3893 (**1993**).
20. Y. H. Shih and A. V. Sergienko. *Phys. Rev. A*, 50, 2564 (**1994**).
21. P. G. Kwiat, K. Mattle, H. Weinfurter, A. Zeilinger, A. V. Sergienko, and Y. Shih. *Phys. Rev. Lett.*, 75, 4337 (**1995**).
22. N. Gisin, G. Ribordy, W. Tittel, and H. Zbinden. *Rev. Mod. Phys.*, 74, 145 (**2002**).
23. R. Loudon, The Quantum Theory of Light, 3rd ed., Oxford University Press, Oxford, U.K. (**2000**).
24. H. J. Carmichael. *Phys. Rev. Lett.*, 55, 2790 (**1985**).
25. J. McKeever, A. Boca, A. D. Boozer, R. Miller, J. R. Buck, A. Kuzmich, and H. J. Kimble. *Science*, 303, 1992 (**2004**).
26. B. Lounis and W. E. Moerner. *Nature*, 407, 491 (**2000**).
27. C. Kurtsiefer, S. Mayer, P. Zarda, and H. Weinfurter. *Phys. Rev. Lett.*, 85, 290 (**2000**).
28. J. I. Gonzalez, Tae-Hee Lee, M. D. Barnes, Y. Antoku, and R. M. Dickson. *Phys. Rev. Lett.*, 93, 147402 (**2004**).
29. B. Lounis and W. E. Moerner. *Nature*, 407, 491 (**2000**).
30. P. Michler, A. Imamoglu, M. D. Mason, P. J. Carson, G. F. Strouse, and S. K. Buratto. *Nature*, 406, 968 (**2000**).
31. G. Messin, J. P. Hermier, E. Giacobino, P. Desbiolles, and M. Dahan. *Opt. Lett.*, 26, 1891 (**2001**).
32. P. Michler, A. Kiraz, C. Becher, W. V. Schoenfeld, P. M. Petroff, L. Zhang, E. Hu, and A. Imamoglu. *Science*, 290, 2282 (**2000**).
33. C. Santori, M. Pelton, G. Solomon, Y. Dale, and Y. Yamamoto. *Phys. Rev. Lett.*, 86, 1502 (**2001**).
34. E. Moreau, I. Robert, J. M. Gérard, I. Abram, L. Manin, and V. Thierry-Mieg. *Appl. Phys. Lett.*, 79, 2865 (**2001**).
35. A. Kiraz, P. Michler, C. Becher, B. Gayral, A. Imamoglu, L. Zhang, E. Hu, W. V. Schoenfeld, and P. M. Petroff. *Phys. Rev. B*, 63, 121312 (**2001**).
36. Z. Yuan, B. E. Kardynal, R. M. Stevenson, A. J. Shields, C. J. Lobo, K. Cooper, N. S. Beattie, D. A. Ritchie, and M. Pepper. *Science*, 295, 102 (**2002**).
37. V. Zwiller, T. Aichele, W. Seifert, J. Persson, and O. Benson. *Appl. Phys. Lett.*, 82, 1509 (**2003**).
38. K. Takemoto, Y. Sakuma, S. Hirose, T. Usuki, N. Yokoyama, T. Miyazawa, M. Takatsu, and Y. Arakawa. *Jpn. J. Appl. Phys.*, 43, 993 (**2004**).
39. T. Miyazawa, K. Takemoto, Y. Sakuma, S. Hirose, T. Usuki, N. Yokoyama, M. Takatsu, and Y. Arakawa. *Jpn. J. Appl. Phys.*, 44, L620 (**2005**).
40. X. Brokmann, E. Giacobino, M. Dahan, and J. P. Hermier. *Appl. Phys. Lett.*, 85, 712 (**2004**).
41. C. Couteau, S. Moehl, F. Tinjod, J. M. Gérard, K. Kheng, H. Mariette, J. A. Gaj, R. Romestain, and J. P. Poizat. *Appl. Phys. Lett.*, 85, 6251 (**2004**).
42. C. Santori, S. Götzinger, Y.Yamamoto, S. Kako, K. Hoshino, and Y. Arakawa. *Appl. Phys. Lett.*, 87, 051916 (**2005**).
43. R. M. Stevenson, R. J. Young, P. Atkinson, K. Cooper, D. A. Ritchie, and A. J. Shields. *Nature* 439, 179 (**2006**).
44. C. Z. Peng, T. Yang, X. H. Bao, J. Zhang, X. M. Jin, F. Y. Feng, B. Yang, J. Yang, J. Yin, Q. Zhang, N, Li, B. L. Tian, and J. W. Pan. *Phys. Rev. Lett.*, 94, 150501 (**2005**).
45. R. J. Hughes, J. E. Nordholt, D. Derkace, and C. G. Peterson. *New J. Phys.* 4, 43 (**2002**).
46. J. E. Nordholt, R. J. Hughes, G. L. Morgan, C. G. Peterson, and C. C. Wipf. *Proc. SPIE*, 4635, 116 (**2002**).

47. W. T. Buttler, R. J. Hughes, P. G. Kwiat, S. K. Lamoreaux, G. G. Luther, G. L. Morgan, J. E. Nordholt, C. G. Peterson, and C. M. Simmons. *Phys. Rev. Lett.*, 81, 3282 (**1998**).
48. J. G. Rarity, P. R. Tapster, P. M. Gorman, and P. Knight. *New J. Phys.*, 4, 82 (**2002**).
49. B. C. Jacobs and J. D. Franson. *Optics Lett.*, 21, 1854 (**1996**).
50. N. Gisin, G. Ribordy, W. Tittel, and H. Zbinden. *Rev. Mod. Phys.*, 74, 145 (**2002**).
51. C. Kurtsiefer, P. Zarda, M. Halder, H. Weinfurter, P. M. Gorman, P. R. Tapster, and J. G. Rarity. *Nature*, 419, 450 (**2002**).
52. M. Aspelmeyer, H. R. Böhm, T. Gyatso, T. Jennewein, R. Kaltenbaek, M. Lindenthal, G. M. Terriza, A. Poppe, K. Resch, M. Taraba, R. Ursin, P. Walther, and A. Zeilinger. *Science*, 301, 621 (**2003**).
53. S. Fafard, K. Hinzer, S. Raymond, M. Dion, J. McCaffery, Y. Feng, and S. Charbonneau. *Science*, 274, 1350 (**1996**).
54. A. F. Tsatsul'nikov, A. Yu. Egorov, P. S. Kop'ev, A. R. Kovsh, N. N. Ledentsov, M. V. Maximov, A. A. Suvorova, V. M. Ustinov, B.V. Volovik, A. E. Zhukov, M. Grundmann, D. Bimberg, and Z. I. Alferov. *Appl. Surf. Sci. 123/124*, 381 (**1998**).
55. K. Hinzer, P. Hawrylak, M. Korkusinski, and S. Fafard, M. Bayer, O. Stern, A. Gorbunov, and A. Forchel. *Phys. Rev. B*, 63, 075314 (**2001**).
56. T. Yokoi, S. Adachi, H. Sasakura, S. Muto, H. Z. Song, T. Usuki, and S. Hirose. *Phys. Rev. B*, 71, 041307 (**2005**).
57. H. Sasakura, S. Adachi, S. Muto, H. Z. Song, T. Miyazawa, and T. Usuki. *Jpn. J. Appl. Phys.*, 43, 2110 (**2004**).
58. R. Hanbury-Brown and R. Q. Twiss. Nature, 177, 27 (**1956**).
59. V. D. Kulakovskii, G. Bacher, R. Weigand, T. Kümmell, A. Forchel, E. Borovitskaya, K. Leonardi, and D. Hommel. *Phys. Rev. Lett.*, 82, 1780 (**1999**).
60. D. Gammon, E. S. Snow, B. V. Shanabrook, D. S. Katzer, and D. Park. *Phys. Rev. Lett.*, 76, 3005 (**1996**).
61. M. Bayer, G. Ortner, O. Stern, A. Kuther, A. A. Gorbunov, A. Forchel, P. Hawrylak, S. Fafard, K. Hinzer, T. L. Reinecke S. N. Walck, J. P. Reithmaier, F. Klopf, and F. Schäfer. *Phys. Rev. B*, 65, 195315 (**2002**).
62. S. Rodt, A. Schliwa, K. Pötschke, F. Guffarth, and D. Bimberg. *Phys. Rev. B*, 71, 155325 (**2005**).
63. R. J. Young, R. M. Stevenson, A. J. Shields, P. Atkinson, K. Cooper, D. A. Ritchie, K. M. Groom, A. I. Tartakovskii, and M. S. Skolnick. *Phys. Rev. B*, 72, 113305 (**2005**).
64. S. Rodt, R. Heitz, A. Schliwa, R. L. Sellin, F. Guffarth, and D. Bimberg. *Phys. Rev. B*, 68, 035331 (**2003**).
65. B. Patton, W. Langbein, and U. Woggon. *Phys. Rev. B*, 68, 125316 (**2003**).
66. C. Santori, M. Pelton, G. Solomon, Y. Dale, and Y. Yamamoto. *Phys. Rev. Lett.*, 86, 1502 (**2001**).
67. A. Vasanelli, R. Ferreira, and G. Bastard. *Phys. Rev. Lett.*, 89, 216804 (**2002**).
68. Y. Toda, O. Moriwaki, M. Nishioka, and Y. Arakawa. *Phys. Rev. Lett.*, 82, 4114 (**1999**).
69. E. W. Bogaart, J. E. M. Haverkort, T. Mano, T. van Lippen, R. Nötzel, and J. H. Wolter. *Phys. Rev. B*, 72, 195301 (**2005**).
70. J. J. Finley, A. D. Ashmore, A. Lemaître, D. J. Mowbray, M. S. Skolnick, I. E. Itskevich, P. A. Maksym, M. Hopkinson, and T. F. Krauss. *Phys. Rev. B*, 63, 073307 (**2001**).
71. D. V. Regelman, E. Dekel, D. Gershoni, E. Ehrenfreund, A. J. Williamson, J. Shumway, and A. Zunger, W. V. Schoenfeld, and P. M. Petroff. *Phys. Rev. B*, 64, 165301 (**2001**).
72. G. Bester and A. Zunger. *Phys. Rev. B*, 68, 073309 (**2003**).
73. B. Urbaszek, R. J. Warburton, K. Karrai, B. D. Gerardot, P. M. Petroff, and J. M. Garcia. *Phys. Rev. Lett.*, 90, 247403 (**2003**).
74. I. A. Akimov, A. Hundt, T. Flissikowski, and F. Henneberger. *Appl. Phys. Lett.*, 81, 4730 (**2002**).
75. M. Bayer, O. Stern, P. Hawrylak, S. Fafard, and A. Forchel. *Nature*, 405, 923 (**2000**).
76. P. Hawrylak, G. A. Narvaez, M. Bayer, and A. Forchel. *Phys. Rev. Lett.*, 85, 389 (**2000**).
77. C. Santori, G. S. Solomon, M. Pelton, and Y. Yamamoto. *Phys. Rev. B*, 65, 073310 (**2002**).
78. E. Waks, E. Diamanti, and Y. Yamamoto. *New J. Phys.*, 8, 4 (**2006**).
79. B. Lounis, H. A. Bechtel, D. Gerion, P. Alivisatos, and W. E. Moerner. *Chem. Phys. Lett.*, 329, 399 (**2000**).
80. S. Kimura, H. Kumano, M. Endo, I. Suemune, T. Yokoi, H. Sasakura, S. Adachi, S. Muto, H. Z. Song, S. Hirose, and T. Usuki. *Jpn. J. Appl. Phys.*, 44, L793 (**2005**).
81. S. Kimura, H. Kumano, M. Endo, I, Suemune, T. Yokoi, H. Sasakura, S. Adachi, S. Muto, H. Z. Song, S. Hirose, and T. Usuki. *Phys. Stat. Sol. (c)*, 2, 3833 (**2005**).
82. D.V. Regelman, U. Mizrahi, D. Gershoni, and E. Ehrenfreund. *Phys. Rev. Lett.*, 87, 257401 (**2001**).
83. J. J. Finley, P. W. Fry, A. D. Ashmore, A. Lemaître, A. I. Tartakovskii, R. Oulton, D. J. Mowbray, M. S. Skolnick, M. Hopkinson, P. D. Buckle, and P. A. Maksym. *Phys. Rev. B*, 63, 161305 (**2001**).
84. I. A. Akimov, K. V. Kavokin, A. Hundt, and F. Henneberger. *Phys. Rev. B*, 71, 075326 (**2005**).
85. H. Kumano, S. Kimura, M. Endo, I.Suemune, H. Sasakura, S. Adachi, S. Muto, H. Z. Song, S. Hirose, and T. Usuki. *Physica E*, 32, 144 (**2006**).
86. A. Malko, M. H. Baier, E. Pelucchi, D. Y. Oberli, K. Leifer, D. Chek-al-kar, and E. Kapon. *Appl. Phys. Lett.*, 85, 5715 (**2004**).
87. S. Raymond, X. Guo, J. L. Merz, and S. Fafard. *Phys. Rev. B*, 59, 7624 (**1999**).
88. C. H. Bennett, G. Brassard, C. Crépeau, R. Jozsa, A. Peres, and W. K. Wootters. *Phys. Rev. Lett.*, 70, 1895 (**1993**).
89. M. Zukowski, A. Zeilinger, M. A. Horne, and A. K. Ekert. *Phys. Rev. Lett.*, 71, 4287 (**1993**).
90. H.-J. Briegel, W. Dür, J. I. Cirac, and P. Zoller. *Phys. Rev. Lett.*, 81, 5932 (**1998**).
91. K. Edamatsu, G. Oohata, R. Shimizu, and T. Itoh. *Nature*, 431, 167 (**2004**).
92. I. Favero, G. Cassabois, C. Voisin, C. Delalande, Ph. Roussignol, R. Ferreira, C. Couteau, J. P. Poizat, and J. M. Gérard. *Phys. Rev. B*, 71, 233304 (**2005**).
93. P. Borri, W. Langbein, U. Woggon, V. Stavarache, D. Reuter, and A. D. Wieck. *Phys. Rev. B*, 71, 115328 (**2005**).
94. H. Gotoh, H. Ando, H. Kamada, A. C. Pirson, and J. Temmyo. *Appl. Phys. Lett.*, 72, 1341 (**1998**).
95. M. Paillard, X. Marie, P. Renucci, T. Amand, A. Jbeli, and J. M. Gérard. *Phys. Rev. Lett.*, 86, 1634 (**2001**).
96. R. M. Stevenson, R. M. Thompson, A. J. Shields, I. Farrer, B. E. Kardynal, D. A. Ritchie, and M. Pepper. *Phys. Rev. B*, 66, 081302 (**2002**).
97. C. Santori, D. Fattal, M. Pelton, G. S. Solomon, and Y. Yamamoto. *Phys. Rev. B*, 66, 045308 (**2002**).
98. S. M. Ulrich, S. Strauf, P. Michler, G. Bacher, and A. Forchel. *Appl. Phys. Lett.*, 83, 1848 (**2003**).
99. A. Kiraz, S. Fälth, C. Becher, B. Gayral, W. V. Schoenfeld, P. M. Petroff, L. Zhang, E. Hu, and A. Imamoğlu. *Phys. Rev. B*, 65, 161303 (**2002**).
100. S. M. Ulrich, M. Benyoucef, P. Michler, N. Baer, P. Gartner, F. Jahnke, M. Schwab, H. Kurtze, M. Bayer, S. Fafard, Z. Wasilewski, and A. Forchel. *Phys. Rev. B*, 71, 235328 (**2005**).
101. E. Moreau, I. Robert, L. Manin, V. Thierry-Mieg, J. M. Gérard, and I. Abram. *Phys. Rev. Lett.*, 87, 183601 (**2001**).
102. T. Watanuki, S. Adachi, H. Sasakura, and S. Muto. *Appl. Phys. Lett.*, 86, 063114 (**2005**).
103. M. Pelton, C. Santori, J. Vučković, B. Zhang, G. S. Solomon, J. Plant, and Y. Yamamoto. *Phys. Rev. Lett.*, 89, 233602 (**2002**).
104. A. Kress, F. Hofbauer, N. Reinelt, M. Kaniber, H. J. Krenner, R. Meyer, G. Böhm, and J. J. Finley. *Phys. Rev. B*, 71, 241304(R) (**2005**).
105. D. Englund, D. Fattal, E. Waks, G. Solomon, B. Zhang, T. Nakaoka, Y. Arakawa, Y. Yamamoto, and J. Vučković. *Phys. Rev. Lett.*, 95, 013904 (**2005**).